

# Salt-Dependent Aggregation and Assembly of *E coli*-Expressed Ferritin

Wei Sun<sup>1</sup>, Chengfeng Jiao<sup>1</sup>, Yue Xiao<sup>1</sup>, Luwei Wang<sup>1</sup>,  
Cheng Yu<sup>1</sup>, Jialin Liu<sup>1</sup>, Yongli Yu<sup>2</sup>, and Liying Wang<sup>1</sup>

Dose-Response:  
An International Journal  
January-March 2016:1-6  
© The Author(s) 2016  
Reprints and permission:  
sagepub.com/journalsPermissions.nav  
DOI: 10.1177/1559325816632102  
dos.sagepub.com



## Abstract

Ferritin, with the primary function of iron storage, is a nearly ubiquitous protein found in most living organisms. Our recent investigations suggest that ferritin can assemble nanoparticles. So we use ferritin as a novel type of delivery vehicle for recombinant epitope vaccines. And, we found that ferritin form nonnative aggregates depended sensitively on NaCl concentrations. Here, we report that ferritin is an ion-sensitive protein and has the attribute of salt-dependent aggregation. Our results indicate that recombinant ferritin can be released as a soluble form from *Escherichia coli* at low NaCl concentrations ( $\leq 50$  mmol/L). Moreover, this result affords us to confirm a proper self-assembling solution for soluble ferritin or other ferritin-based fusion proteins to assemble nanoparticles.

## Keywords

ferritin, nanoparticles, salt-dependent, aggregation, self-assembling

## Introduction

Ferritins are a family of proteins found in all species, which function primarily in ion sequestration. The ferritin protein family can self-assemble into protein cages of 2 types: maxi-ferritin and mini-ferritin.<sup>1</sup> Composed of 24 subunits, maxi-ferritin form a spherical-like structure with external and internal diameters of 12 and 8 nm, respectively.<sup>2</sup> This unique architecture promises the 24-subunit ferritin a suitable character when utilized as antigen nanocarrier. Whether fused epitopes can be exposed on the surface of antigen carrier is a critical factor of endowing a protein to be a good antigen delivery agent. One of the successful cases of ferritin used as antigen carrier is a ferritin-HA fusion protein, which can spontaneously assemble and delicately form 8 trimeric viral spikes on its surface.<sup>3</sup>

Various nanotechnologies have been widely exploited for drug delivery, and recently, ferritin-based nanoparticles are drawing more and more attention.<sup>4-17</sup> In particular, self-assembly-based technology has been the subject of intense study in drug delivery.<sup>1,9</sup> Considering the application as nanocages vehicle of ferritin, different expression systems are used to acquire it. Ferritin and ferritin-based fusion proteins can all successfully self-assemble into nanoparticles after expressed in mammalian cells, fungus,<sup>14,18</sup> and *Escherichia coli*.<sup>12,19</sup> As has been known, ferritin nanocage has an interesting feature: The nanocage can be broken down into subunits in an acidic

environment (pH = 2.0), and such process is reversible. When the pH is tuned back to neutral (pH 7.2), the ferritin subunits will be reconstituted into a nanocage structure<sup>5,20</sup> and almost in an intact fashion.<sup>13,21</sup>

Because of no need for posttranslational modifications and the ubiquitous feature of ferritin, in our study, we preferred to utilize *E coli*, the versatile host for the production of heterologous proteins, to express ferritin and developed a ferritin-based fusion protein-expressed platform. When we cloned and expressed ferritin and its fusion proteins in *E coli*, it was found that ferritin aggregated in the precipitate. And, the aggregates were noncovalent, as evidenced by their rapid dissociation in the presence of urea. In the process of exploring aggregated reason, the present work provides the first study of the reversible phase behavior for nonnative aggregates of ferritin as a function of NaCl concentration. We found that NaCl in the

<sup>1</sup> Department of Molecular Biology, College of Basic Medicine, Jilin University, Changchun, China

<sup>2</sup> Department of Immunology, College of Basic Medicine, Jilin University, Changchun, China

## Corresponding Author:

Liying Wang, College of Basic Medical Sciences, Jilin University, 126 Xinmin Street, Changchun 130021, China.

Email: wlying@jlu.edu.cn



lysis buffer was related to the solubility and self-assembly character of ferritin.

## Materials and Methods

### *Cloning and Inducible Expression of Ferritin Fusion Protein*

Based on the sequence of ferritin in *Helicobacter pylori* from the NCBI database (GenBank accession number: AE001439.1), a pair of primers, Fer-f1 (5'-GGATCC GGCGGT TCAAAA GACATC ATTAAG TTGC-3') and Fer-r1 (5'-CTCGAG AGATTT CCTGCT TTTAGC GATC-3'), was designed to amplify a partial DNA fragment. Polymerase chain reaction (PCR) amplification was performed using the complementary DNA template from *H pylori* (HPss1; 94°C for 5 minutes, 94°C for 45 seconds, 55°C for 1 minute, and 72°C for 1 minute, 30 cycles, followed by 1 cycle of 72°C for 10 minutes and 1 cycle of 4°C to hold). The PCR products were isolated on 1.2% agarose gel and purified using a gel extraction kit (E.Z.N.A, USA). The purified PCR products were inserted into the pET-28a plasmid (Novagen) using T4 DNA ligase (Takara) after cleaving with BamHI and XhoI (Takara). For the purpose of purification, the coding sequence of His-tag was constructed at both ends of the constructed coding genes.

### *Bacterial Ultrasonic Lysis and Polyacrylamide Gel Electrophoresis*

The recombinant pET-28a/ferritin plasmid was transformed into the *E coli* BL21 (DE3) strain. The ferritin *E coli* BL21 (DE3) cells were cultured in LB media with 0.5% kanamycin at 37°C and induced at an OD600 of 0.6 with 0.4% isopropyl- $\beta$ -D-thiogalactopyranoside for 3 hours at 37°C. The final culture was then harvested by centrifugation at 8000g for 10 minutes at 4°C, and the pellet was collected. Then, the pellet was resuspended in LB medium (1% NaCl, 1% Typone, 0.5% yeast extract)/lysis buffer (20 mmol/L Tris, 50 mmol/L NaCl, 1 mmol/L EDTA, pH 7.6) and different concentrations of NaCl solution (0, 50, 100, 170, and 300 mmol/L), respectively. The cells were lysed by sonication (input power 5 seconds/600 W, interval 10 seconds, 40 cycles) and then centrifuged at 10 000g for 15 minutes at 4°C. The supernatant and precipitate were analyzed by sodium dodecyl sulfate polyacrylamide gel electrophoresis (SDS-PAGE). All sodium dodecyl sulfate-stained gels were scanned with high-resolution scanner (Canon Scanner 110). Gel images were analyzed using Magic Chemi 1D software (Wealtec). For optimal clarity, protein bands were detected by adjusting parameters. The data for the bands were generated from technical triplicates.

### *Ferritin Purification*

The supernatant of ferritin cell lysis was loaded into 3 mL of Ni-NTA His-Bind resin (Merck Millipore). The column was washed first with 10 column volumes of buffer A (20 mmol/L

Tris-HCl, 50 mmol/L NaCl, 20 mmol/L imidazole, 0.03% Tween 80, pH 7.6) and then eluted in 2 mL buffer B (20 mmol/L Tris-HCl, 50 mmol/L NaCl, 500 mmol/L imidazole, 0.03% Tween 80, pH 7.6). The eluted solution was loaded into Sephadex G-25 (Sigma), and the solution was finally washed by buffer C (20 mmol/L Tris-HCl, 50 mmol/L NaCl, 0.03% Tween 80, pH 7.6).<sup>22,23</sup>

### *Ferritin Solution Dialysis and Ultraviolet-Visible Spectrometry Observation*

To make sure the purified ferritin is retained in monomer form, pH of buffer C was regulated to 2.0. Then, the denatured protein was evenly divided and dialyzed in buffer D (20 mmol/L Tris-HCl, 0.03% Tween 80, pH 7.6, 50/100/170/300 mmol/L NaCl) at 4°C.<sup>22,23</sup> After dialysis, the protein solutions that contain different NaCl concentrations were placed in 1-cm<sup>2</sup> quartz cuvettes to monitor optical density. Optical density was taken at  $\lambda = 650$  nm.

### *Transmission Electron Microscopy*

The solutions of ferritin in buffer C and buffer D with 50 to 300 mmol/L NaCl were prepared for transmission electron microscopy (TEM) measurements. Several microliters of solutions were put on the carbon film-coated mesh for TEM, and excessive solution was removed. The samples were negatively stained by 1% aurothioglucose and observed by TEM.

## Results

### *Effect of Different Ultrasonic Medium on the Character of Ferritin*

To acquire ferritin in *E coli*, samples were treated by ultrasonic with LB medium. Then, the lysate was centrifuged. The supernatant and precipitate were analyzed by SDS-PAGE. It was found that the ferritin emerged as a polymeride in the precipitate (Figure 1). Ferritin is a protein that naturally forms nanoparticles. It should be soluble in the supernatant. Then, we change the ultrasonic medium to lysis buffer (20 mmol/L Tris-HCl, 150 mmol/L NaCl, 1 mmol/L Na<sub>2</sub> EDTA, 1 mmol/L ethylene glycol tetraacetic acid [EGTA], 1% Trion X-100, 2.5 mmol/L sodium pyrophosphate, 1 mmol/L glycerophosphate, 1 mmol/L Na<sub>3</sub>VO<sub>4</sub>, 1  $\mu$ g/mL leupeptin) and repeated the above procedures. Interestingly, this time ferritin was in the supernatant (Figure 1). These data indicated that components (1% Typone, 0.5% yeast extract, 1% NaCl) in the LB medium cause ferritin in the precipitate. Then, we use 1% Typone, 0.5% yeast extract, and 1% NaCl (170 mmol) as ultrasonic medium to lyse the bacteria, respectively. The results showed that Typone and yeast extract had little effect on the solubility of ferritin, and 1% NaCl (170 mmol) cause 50% of ferritin in the precipitate. In contrast, we assayed the character of flagellin and its soluble expression both with LB medium and lysis buffer. Meanwhile, we assayed the character of VP1

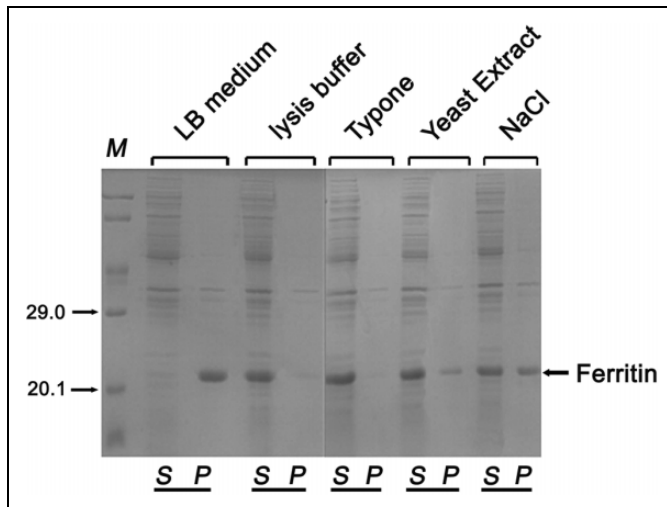


**Figure 1.** SDS-PAGE analysis of ferritin distribution between soluble and aggregation after bacterial cell ultrasonic disruption. Note. Ferritin was overexpressed in the *E. coli* BL21 (DE3) strain. 5 mediums were studied as ultrasonic buffer: LB medium, lysis buffer, 1%Typone, 5%Yeast Extract and 1%NaCl. Here the soluble and aggregation of ferritin can be observed. Higher percentage of the aggregates can be observed in the insoluble sample after ultrasonic disruption ( $n=3$ ). LB medium-insoluble form after sonication. Lysis buffer-soluble form after sonication. 1% Typone- soluble form after sonication. 5% Yeast Extract-soluble form after sonication. 1%NaCl- insoluble form after sonication. S-supernatant & P-precipitate.

**Table 1.** SDS-PAGE Data of Ferritin Distribution Between Soluble and Insoluble With Control Protein.

Protein	Medium				
	LB Medium	Lysis Buffer	1% Typone	5% Yeast Extract	1% NaCl
Ferritin	-	+	+	+	-
VPI	-	-	-	-	-
Flagellin	+	+	+	+	+

Abbreviations: SDS-PAGE, sodium dodecyl sulfate polyacrylamide gel electrophoresis; +, soluble; -, insoluble.

as negative control, which emerged in precipitate both with LB medium and lysis buffer, and we assayed the character of flagellin as positive control, which emerged in supernate both with LB medium and lysis buffer (Table 1). These results clearly demonstrate that ferritin is an ion-sensitive protein.

### Effect of NaCl Concentrations on the Character of Ferritin

Ionic strength is believed to play a key role in the assembly and stability of protein. To investigate this, ultrasonic medium were changed with various NaCl concentrations (0, 50, 100, 170, 300 mmol/L) in lysis buffer (20 mmol/L Tris-HCL, 1 mmol/L  $\text{Na}_2$  EDTA, 1 mmol/L EGTA, 1% Trion X-100, 2.5 mmol/L sodium pyrophosphate, 1 mmol/L glycerophosphate, 1 mmol/L

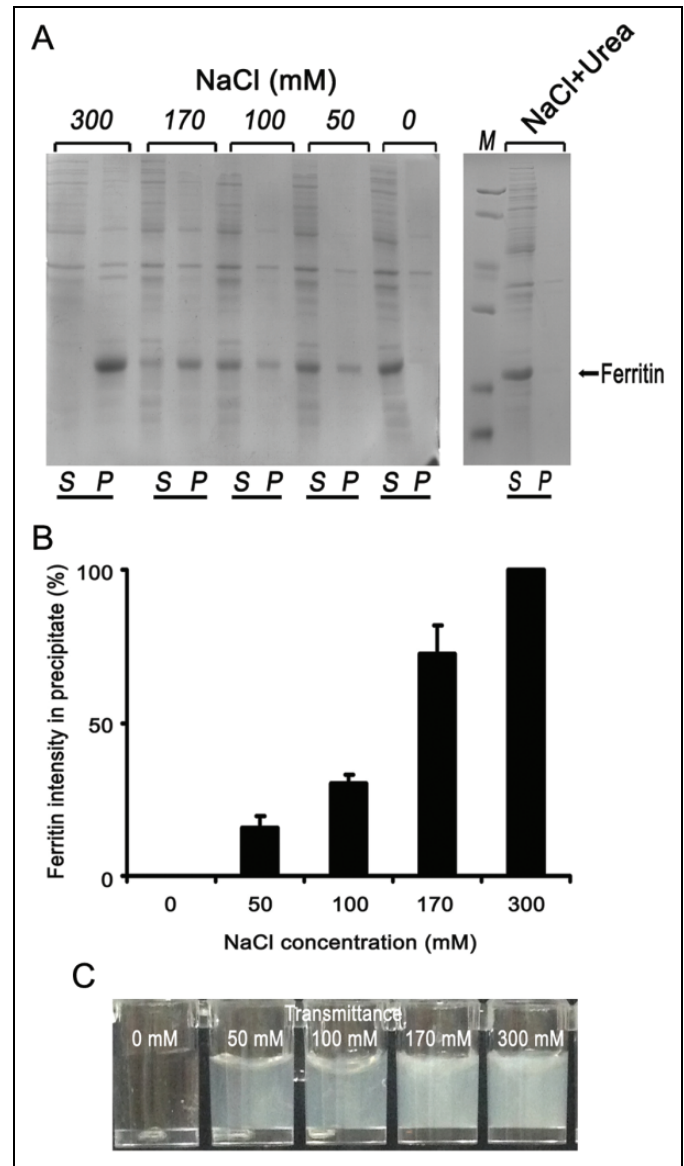


**Figure 2.** SDS-PAGE analysis of NaCl concentrations on the character of Ferritin.

Note. A. Ferritin was overexpressed in the *E. coli* BL21 (DE3) strain. Different concentrations of NaCl were studied: 0, 50, 100, 170, 300 mM. Here the soluble and precipitate of ferritin can be observed. 100% of ferritin protein was released as soluble form at 0 mM NaCl. About 50% of ferritin was in the precipitate at 50-170 mM NaCl. Ferritin protein was as aggregation form at higher concentrations of NaCl (300 mM). When 0.5 M urea exist in the solution, even if the concentration of NaCl is 500 mM, ferritin released as soluble form. S-supernatant & P-precipitate. B. Different concentrations of NaCl illustrating the enhanced amount of precipitate Ferritin aggregates ( $n=3$ ). C. Representative examples for different concentration of NaCl. Approximate percent transmission values are indicated on each digital image.

$\text{Na}_3\text{VO}_4$ , 1  $\mu\text{g}/\text{mL}$  leupeptin; Figure 2A and B). The data showed that approximately 100% of ferritin protein was released as a soluble form at 0 mmol/L NaCl. And almost 50% of ferritin was in the precipitate at 50 to 170 mmol/L NaCl. However, ferritin protein was in aggregate form at higher

concentrations of NaCl (300 mmol/L). We still assayed flagellin and VP1 as controls, and approximately 100% of flagellin was released as soluble form at 300 mmol/L NaCl. The epitopes of foot-and-mouth disease viruses (FMDV) have been under extensive investigation. VP1 capsid protein has been revealed to carry critical epitopes for inducing immune responses, including 1 major B-cell epitope and 2 T-cell epitopes. The most dominant B-cell epitope in FMDV spans residues 141 to 160 aa and is highly exposed on the surface of the virion. Antibody responses against the loop are able to neutralize FMDV. Our laboratory has constructed the recombinant protein of VP1, and most of it was expressed as inclusion bodies in *E coli*.<sup>11</sup> And flagellin is the component antigen of the flagellar filament.<sup>11</sup> This protein is exposed on the bacterial surface, is available to B cells, can be expressed at high levels, and is a significant target of the T-cell response to STM.<sup>7</sup> Furthermore, our laboratory has constructed the recombinant protein of flagellin, and it was a soluble expression in *E coli*.<sup>11</sup> These results showed that ferritin has the attribute of salt-dependent aggregation. The series of digital images in Figure 2C shows representative examples for different concentrations of NaCl to help align the percentage transmission values to what is apparent from visible observation as the titrations proceed.

#### Percentage of Transmission of Ferritin in Different Concentrations of NaCl Solutions

We used NaCl as the precipitating agent for different ferritin concentrations. It shows that the location of the salt-dependent cloud points is sensitive to the total protein concentration. In that, higher protein concentration makes the transition occur more readily, that is, at lower salt concentrations. Figure 3 shows sharp cloud-point transitions, akin to the forward titrations of pH in Figure 2C. A striking feature of Figures 2C and 3 is the sensitivity of the location of the transition to the identity of ferritin. Physically, this is a major driving force that prevents aggregate coalescence, and phase separation is electrostatic repulsions between the aggregate molecules, as was suggested previously based on isolated results for aggregate cloud points.

The series of digital images in Figure 3 shows representative examples for different points along the forward titration curve for the buffer-only condition to help align the percentage transmission values to what is apparent from visible observation as the titrations proceed.

#### Electromagnetic Wave Absorption Properties of Ferritin Nanocomposites

To characterize the morphologies of ferritin nanoparticles at lower and higher NaCl concentrations, samples were examined by TEM. The nanoparticles with diameters ranging from 10.5 to 13 nm (mean 12 nm) can be observed in the samples treated at lower NaCl concentrations ( $\leq 50$  mmol/L), whereas these structures were not detected in the samples treated at higher NaCl concentrations (100-300 mmol/L);

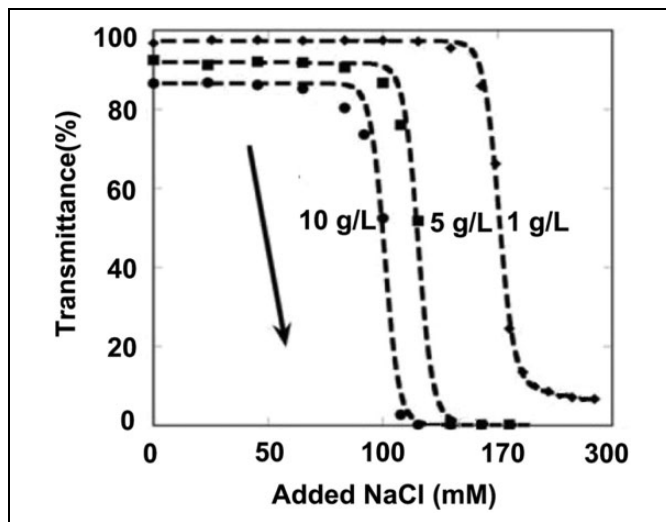


**Figure 3.** NaCl titration for cloud points of Ferritin aggregates at three different total aggregate concentrations: 10 mg/ml (circles), 5 mg/ml (squares), and 1 mg/ml (diamonds).

Note. The arrow indicates the direction of the titration.

Figure 4). These results clearly demonstrated that lower NaCl concentrations ( $\leq 50$  mmol/L) could promote ferritin form nanoparticles.

#### Discussion

The structural properties, especially the capacity of loading foreign peptides, make ferritin a powerful potential nanoplat-form on which to construct multifunctional nanofusion proteins.<sup>24,25</sup> The advantages of ferritin-based fusion protein as vaccine exist in 2 aspects: the recognition frequency of peptide is amplified and the volume of fusion protein is big enough to afford a strong immunogenicity, which endows it the great potential to be a successful vaccine. In our research, both ferritin itself and ferritin-based fusion proteins can assemble into nanoparticles, proving foundation for fusion proteins to be effective vaccines.

During the process of bacterial ultrasonic crack, we found that one protein, no matter what kind of ultrasonic medium (LB or lysis buffer) was used, would always have the same result. If ferritin emerged in supernatant, it was seemed as soluble expressed, such as flagellin.<sup>10,26</sup> If ferritin was in precipitate, it was seemed as aggregated expressed, such as VP1.<sup>15,27</sup> So, when little scale tests were did to see the solubility of one protein expressed in *E coli* in our laboratory, bacteria in LB were brought to do the ultrasonic crack directly for operating convenience usually. With LB as ultrasonic medium directly, it was found that ferritin as a polymeride emerged in the precipitate.

Considering the ubiquitous feature of ferritin, referring to the papers related to ferritin expression,<sup>28,29</sup> which reported that ferritin was soluble expressed in *E coli*, we guessed there must be some verstellbar elements that could be altered to get soluble ferritin. We adjusted nutrition of culture medium, pH value, induction temperature, and finally focus on the

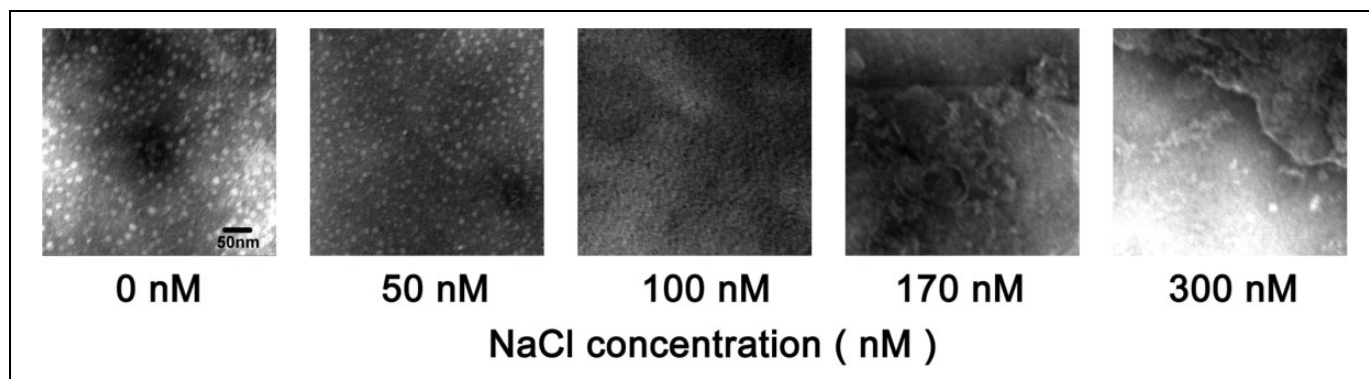


**Figure 4.** Electron micrographs of ferritin preparations.

Note. The protein solutions that contain different NaCl concentration (0 - 300 mM) were negatively stained by 1% aurothioglucose and viewed using a TEM operating at 80 KV.

ultrasonic medium. After decreased concentration of NaCl in ultrasonic medium, ferritin was soluble in the supernatant. The results suggested that being different from other proteins, ferritin was so sensitive to ionic strength in environment. If using LB as the ultrasonic medium, it would lead to a false appearance of aggregated expression in *E coli*. We then designed a series concentration of NaCl solvated in lysis buffer, which are 300 mmol/L, 170 mmol/L, 100 mmol/L, 50 mmol/L, and 0 mol/L separately. The concentration 170 mmol/L is equivalent to 1% quality percentage concentration of NaCl, which is the same composition in LB, trying to recur the same ionic strength of ferritin experienced in LB. Compared with 170 mmol/L, 300 mmol/L is a relatively high concentration for ferritin that would lead it aggregated. The concentration 100 mmol/L is a regular choice for lysis buffer according to the third edition of *Molecular Cloning*.<sup>16,30</sup> NaCl 50 mmol/L is a relatively low concentration for ferritin that would lead it to be soluble. NaCl 0 mmol/L used as blank control. Our results indicated that the concentration of NaCl should be below 100 mmol/L in the purification and assembling process of ferritin-related proteins. The choice of NaCl concentration in our following experiment was 50 mmol/L, which was proven as a good choice for the successful refolding procedure of ferritin itself and ferritin-based fusion proteins. But to those aggregated expression proteins in *E coli*, even if the ionic strength in ultrasonic medium was adjusted, their aggregation state still can't be altered, such as VP1 shown in Figure 1 as negative control.

Salt-protein interactions regulate protein solubility and stability, particularly in the processes of salting out and aggregation. At physiological conditions, triggered by the presence of salt, intramolecular folding events induce the correct peptide formation. Circular dichroism spectroscopy shows that peptides are unfolded at pH 7.4 in the absence of salt. By raising the ionic strength of the solution, electrostatic interactions between charged amino acids within the peptide are screened, and a hydrophobic conformation is adopted. At relatively high salt concentrations, hydrophobic interactions dominate and lead to the precipitation of the chemically

cross-linked polymer chains.<sup>31,32</sup> It is shown that changes in salt concentration induce aggregation not only through the formation of protein intermediates, the peptides, but also through charge screening and various solvation forces. It is the complex interaction between such protein secondary structures and the solvation forces that is responsible for the salt-triggered aggregation.

In the following experiments, we found that when 0.5 mol/L urea exists in the solution, even if the concentration of NaCl is 500 mmol/L, ferritin still be soluble because urea can transform the surface charge distribution of ferritin and improve its solubility. But the 0.5 mol/L urea maybe have slight impact on activity of proteins, so we can try to adjust NaCl concentration to a proper range (<100 mmol/L) to promote ferritin self-assembling process without the existence of urea. The attribute of salt-dependent aggregation of ferritin affords us a theoretical basis in finding a proper self-assembling solution for ferritin and other ferritin-based fusion proteins. It also gives us a reminder that some empirical methods maybe lead to a false appearance in the science research.

#### Declaration of Conflicting Interests

The author(s) declared no potential conflicts of interest with respect to the research, authorship, and/or publication of this article.

#### Funding

The author(s) disclosed receipt of the following financial support for the research, authorship, and/or publication of this article: This work was supported by the National Nature Scientific Foundation of China (81200145).

#### References

1. Zhang Y, Orner BP. Self-assembly in the ferritin nano-cage protein superfamily. *Int J Mol Sci*. 2011;12(8):5406-5421.
2. MaHam A, Tang Z, Wu H, Wang J, Lin Y. Protein-based nanomedicine platforms for drug delivery. *Small*. 2009;5(15):1706-1721.

3. Kanekiyo M, Wei C-J, Yassine HM, et al. Self-assembling influenza nanoparticle vaccines elicit broadly neutralizing H1N1 antibodies. *Nature*. 2013;499(7456):102-106.
4. Chang L, Howdyshell M, Liao WC, et al. Magnetic tweezers-based 3D microchannel electroporation for high-throughput gene transfection in living cells. *Small*. 2015;11(15):1818-1828.
5. Chenguang Z, Zhaogang Y, Lesheng T. Nanomedicine based on nucleic acids: pharmacokinetic and pharmacodynamic perspectives. *Curr Pharm Biotechnol*. 2014;15(9):829-838.
6. Engman C, Wen Y, Meng WS, Bottino R, Trucco M, Giannoukakis N. Generation of antigen-specific Foxp3 + regulatory T-cells in vivo following administration of diabetes-reversing tolerogenic microspheres does not require provision of antigen in the formulation. *Clin Immunol*. 2015;160(1):103-123.
7. Saunders MJ, Liu W, Szent-Gyorgyi C, et al. Engineering fluorogen activating proteins into self-assembling materials. *Bioconjugate Chem*. 2013;24(5):803-810.
8. Song J, Xie J, Li C, et al. Near infrared spectroscopic (NIRS) analysis of drug-loading rate and particle size of risperidone microspheres by improved chemometric model. *Int J Pharm*. 2014;472(1-2):296-303.
9. Wen Y, Kolonich HR, Kruszewski KM, Giannoukakis N, Gawalt ES, Meng WS. Retaining antibodies in tumors with a self-assembling injectable system. *Mol Pharm*. 2013;10(3):1035-1044.
10. Wen Y, Meng WS. Recent in vivo evidences of particle-based delivery of small-interfering RNA (siRNA) into solid tumors. *J Pharm Innov*. 2014;9(2):158-173.
11. Wen Y, Roudebush SL, Buckholtz GA, et al. Coassembly of amphiphilic peptide EAK16-II with histidinylated analogues and implications for functionalization of  $\beta$ -sheet fibrils in vivo. *Biomaterials*. 2014;35(19):5196-5205.
12. Xie J, Teng L, Yang Z, et al. A polyethylenimine-linoleic acid conjugate for antisense oligonucleotide delivery. *BioMed Res Int*. 2013;2013:710502.
13. Xinmei W, Xiaomeng H, Zhaogang Y, et al. Targeted delivery of tumor suppressor microRNA-1 by transferrin-conjugated lipopolyplex nanoparticles to patient-derived glioblastoma stem cells. *Curr Pharm Biotechnol*. 2014;15(9):839-846.
14. Yang Z, Yu B, Zhu J, et al. A microfluidic method for synthesis of transferrin-lipid nanoparticles loaded with siRNA LOR-1284 for therapy of acute myeloid leukemia. *Nanoscale*. 2014;6(16):9742-9751.
15. Zheng Y, Wen Y, George AM, et al. A peptide-based material platform for displaying antibodies to engage T cells. *Biomaterials*. 2011;32(1):249-257.
16. Wen Y, Liu W, Bagia C, et al. Antibody-functionalized peptidic membranes for neutralization of allogeneic skin antigen-presenting cells. *Acta Biomaterialia*. 2014;10(11):4759-4767.
17. Yu B, Wang X, Zhou C, et al. Insight into mechanisms of cellular uptake of lipid nanoparticles and intracellular release of small RNAs. *Pharm Res*. 2014;31(10):2685-2695.
18. Vakdevi V, Sashidhar RB, Deshpande V. Purification and characterization of mycoferritin from *Aspergillus flavus* MTCC 873. *Indian J Biochem Biophys*. 2009;46(5):360-365.
19. Todd TJ, Zhen Z, Xie J. Ferritin nanocages: great potential as clinically translatable drug delivery vehicles? *Nanomedicine*. 2013;8(10):1555-1557.
20. Kang H-T, Linton JA, Shim J-Y. Serum ferritin level is associated with the prevalence of metabolic syndrome in Korean adults: The 2007–2008 Korean National Health and Nutrition Examination Survey. *Clin Chim Acta*. 2012;413(5-6):636-641.
21. Lee S, Kim JW, Shin S, et al. HFE gene mutations, serum ferritin level, transferrin saturation, and their clinical correlates in a Korean Population. *Digest Dis Sci*. 2009;54(4):879-886.
22. Fang M, Wang H, Tang T, Zhao P, Du J, Guo S, et al. Single immunization with a recombinant multiple-epitope protein induced protection against FMDV type Asia 1 in cattle. *Int Immunopharmacol*. 2015;28(2):960-966.
23. Wei H, Fang M, Wan M, et al. Influence of hydrophilic amino acids and GC-content on expression of recombinant proteins used in vaccines against foot-and-mouth disease virus in *Escherichia coli*. *Biotechnol Lett*. 2014;36(4):723-729.
24. Butts CA, Swift J, Kang SG, et al. Directing noble metal ion chemistry within a designed ferritin protein. *Biochemistry*. 2008;47(48):12729-12739.
25. Gao Y, Hou C, Zhou L, et al. A dual enzyme microgel with high antioxidant ability based on engineered seleno-ferritin and artificial superoxide dismutase. *Macromol Biosci*. 2013;13(6):808-816.
26. Zhang H, Liu L, Wen K, et al. Chimeric flagellin expressed by *Salmonella typhimurium* induces an ESAT-6-specific Th1-type immune response and CTL effects following intranasal immunization. *Cell Mol Immunol*. 2011;8(6):496-501.
27. Stubenrauch K, Bachmann A, Rudolph R, Lilie H. Purification of a viral coat protein by an engineered polyionic sequence. *J Chromatogr B Biomed Sci Appl*. 2000;737(1-2):77-84.
28. Fukuzawa T. Ferritin H subunit gene is specifically expressed in melanophore precursor-derived white pigment cells in which reflecting platelets are formed from stage II melanosomes in the periodic albino mutant of *Xenopus laevis*. *Cell Tissue Res*. 2015;361(3):733-744.
29. Ruzzenenti P, Asperti M, Mitola S, et al. The ferritin-heavy-polyptide-like-17 (FTHL17) gene encodes a ferritin with low stability and no ferroxidase activity and with a partial nuclear localization. *Biochim Biophys Acta*. 2015;1850(6):1267-1273.
30. Yang H, Guan H, Yang M, et al. Upregulation of mitochondrial ferritin by proinflammatory cytokines: implications for a role in Alzheimer's disease. *J Alzheimers Dis*. 2015;45(3):797-811.
31. Arosio P, Jaquet B, Wu H, Morbidelli M. On the role of salt type and concentration on the stability behavior of a monoclonal antibody solution. *Biophys Chem*. 2012;168-169:19-27.
32. Yucel U, Peterson DG. Effect of protein–lipid–salt interactions on sodium availability in the mouth and consequent perception of saltiness: as affected by hydration in powders. *J Agric Food Chem*. 2015;63(34):7494-7498.